# Robust GPS-Based Direct Timing Estimation for PMUs

Yuting Ng, *Student Member, IEEE*, Arthur Hsi-Ping Chu and Grace Xingxin Gao, *Senior Member, IEEE*

## BIOGRAPHIES

**Yuting Ng** is a Master's student in the Aerospace Engineering Department at the University of Illinois at Urbana-Champaign. She received her Bachelor's degree, graduating with university honors, from the Electrical and Computer Engineering Department at the same university in 2014. Her research interests are in advanced signal tracking algorithms, remote sensing and controls.

**Arthur Hsi-Ping Chu** is a Master's student in the Electrical and Computer Engineering Department at University of Illinois at Urbana-Champaign. He received his Bachelor's degree in Electrical Engineering from National Taiwan University, Taipei, Taiwan in 2015. His research interests include software engineering and control systems.

**Grace Xingxin Gao** received her B.S. degree in mechanical engineering and her M.S. degree in electrical engineering from Tsinghua University, Beijing, China in 2001 and 2003. She received her PhD degree in electrical engineering from Stanford University in 2008. From 2008 to 2012, she was a research associate at Stanford University. Since 2012, she has been an assistant professor in the Aerospace Engineering Department at University of Illinois at Urbana-Champaign. Her research interests are systems, signals, control, and robotics. She is a senior member of the Institute of Electrical and Electronics Engineers (IEEE) and a member of the Institute of Navigation (ION).

***Abstract*—Phasor Measurement Units (PMUs), also known as synchrophasors, are used to measure the states of the power grid. Their GPS time synchronized readings provide assistance with real-time operations and off-line analysis to improve the reliability and efficiency of the grid. Unfortunately, the GPS signal is weak and vulnerable to jamming, meaconing and spoofing. As such, there is a concern that the GPS-based time synchronization of PMUs may be a potential point of entry for attacks on the power system, resulting in power disturbances and/or outages. To address this concern, we present Direct Timing Estimation (DTE) for the reliable, robust and secure GNSS-based time transfer to PMUs.**

**As a direct method, Direct Timing Estimation (DTE) does not rely on intermediate measurements such as code discriminations and pseudoranges. Instead, it generates timing solutions by operating directly on the raw signal. In this manner, the entire received signal information is utilized, leading to increased robustness in tracking. We developed and implemented DTE on our research platform - PyGNSS. We then conduct realistic simulations, such as jamming and meaconing, based on data collected from field experiments to evaluate the performance of DTE. Through the experiments, we demonstrate the enhanced performance of DTE with respect to conventional algorithms, such as scalar tracking and vector tracking, in hostile situations.**

Yuting Ng and Grace Xingxin Gao are with the Department of Aerospace Engineering; Arthur Hsi-Ping Chu is with the Department of Electrical and Computer Engineering, University of Illinois at Urbana-Champaign, Urbana, IL 61801, USA. E-mail: yng5@illinois.edu, achu11@illinois.edu, gracegao@illinois.edu.

## I. INTRODUCTION

Direct Timing Estimation (DTE) works by Maximum Likelihood Estimation (MLE) of timing, similar to MLE of position in Direct Positioning (DP) or Direct Position Estimation (DPE). MLE operates by searching for the optimal parameter value that maximizes the likelihood of the observation. Applying MLE to DPE, the observation is the entire received signal and the set of parameters to be optimized are the receiver position, clock bias, velocity and clock drift. Each parameter set is used to generate a corresponding signal replica and the correlation amplitude between the signal replica and the received signal gives an indication of the joint likelihood between the underlying parameters and the observation. This process utilizes information from the entire received signal and operates without the use of intermediate measurements, such as pseudorange and carrier phase.

In the case of PMU applications where the known, true position of the static GPS receiver can be accurately and precisely surveyed ahead of time, only the search in the timing domain is required. Thus, the set of parameters to be searched for can be reduced from the receiver position, clock bias, velocity and clock drift to just clock bias and clock drift. This reduces the dimensionality of the problem from eight to two, reducing computational complexity while providing an additional layer of security and robustness.

The rest of the paper is organizes as follows. Section II of the paper describes the DTE receiver architecture. The signal replica is generated from a known receiver position, velocity and the parameter set containing only the clock bias and clock drift. The objective is to search for the timing solution that would maximize the correlation between the signal replica and the received signal. Section III-A of the paper discusses the experiments based on field data. The data was collected using a Universal Software Radio Peripheral (USRP) connected to a Chip-Scale Atomic Clock (CSAC). The experiments, where the receiver was subjected to simulated jamming and meaconing, was conducted in post-processing using our research platform - PyGNSS. Section III-B provides an analysis of the experimental results, demonstrating the viability of DTE and its robustness to hostile situations. Finally, Section IV summarizes the paper.

## II. Direct Timing Estimation

We propose Direct Timing Estimation (DTE) for the secure and robust GPS-based time transfer to PMUs. DTE is based on the concept of a vector correlator, where a signal replica, comprising of all channels in-view, is generated and correlated against the received signal. In section II-A, we begin by describing one of our novel, effective and computationally efficient implementation of the vector correlator. We then discuss our implementation of a joint navigation and tracking Extended Kalman Filter (EKF) that goes well with that implementation of the vector correlator. In section II-B, we further specialize and simplify our implementation of DTE.

### A. DTE with Vector Correlator and Extended Kalman Filter

In DTE, we are searching for the clock bias $X_{c\delta t}$ and clock drift $X_{c\delta \dot{t}}$ parameters that leads to the signal replica having the highest correlation against the received signal. In other words, given the known receiver position $X_{x,y,z}$ and velocity $X_{\dot{x},\dot{y},\dot{z}}$, we are trying to estimate the timing states of the Receiver:

$$\begin{aligned} X &: \text{state vector of Receiver} \\ &= \left[c\delta t, c\dot{\delta t}\right]^T \\ c\delta t &: \text{clock bias } (m) \\ c\dot{\delta t} &: \text{clock drift } (ms^{-1}) \\ c &: \text{speed of light, } 299792458\ (ms^{-1}) \end{aligned} \tag{1}$$

To estimate the unknown timing states of the Receiver, we have to first look at the relationship between the Receiver states and the received signal. We begin by modelling the received GPS signal as follows:

$$\begin{aligned} Y &: \text{model of received GPS signal} \\ &= \sum D^i(t)G^i(f^i_{code,k}t + \phi^i_{code,k})e^{j2\pi(f^i_{carr,k}t+\phi^i_{carr,k})} \end{aligned} \tag{2}$$

$$D^i(t) : \text{databit sequence of the } i^{th} \text{ satellite}$$

$$G^i(t) : \text{L1 C/A code sequence of the } i^{th} \text{ satellite}$$

$$\begin{aligned} f^i_{code,k} &: \text{code frequency of the } i^{th} \text{ satellite} \\ &= f_{C/A} + f_{caid} \times f^i_{dcarr,k} \end{aligned} \tag{3}$$

$$\begin{aligned} \phi^i_{code,k} &: \text{code phase of the } i^{th} \text{ satellite} \\ &= \frac{-f_{C/A}}{c}(\left\|X_{x,y,z,ECI} - X^i_{x,y,z,ECI}\right\| \\ &\quad +(X_{c\delta t} - X^i_{c\delta t})) \end{aligned} \tag{4}$$

$$\begin{aligned} f^i_{carr,k} &: \text{carrier frequency of the } i^{th} \text{ satellite} \\ &= f_{IF} + f^i_{dcarr,k} \end{aligned} \tag{5}$$

$$f_{IF} : \text{intermediate frequency (IF), } (Hz)$$

$$\begin{aligned} f^i_{dcarr,k} &: \text{carrier doppler frequency of the } i^{th} \text{ satellite} \\ &= \frac{-f_{L1}}{c}(-los^i_{x,y,z} \cdot (X_{\dot{x},\dot{y},\dot{z},ECI} \\ &\quad -X^i_{\dot{x},\dot{y},\dot{z},ECI}) + (X_{c\dot{\delta t}} - X^i_{c\dot{\delta t}})) \end{aligned} \tag{6}$$

$$\begin{aligned} los^i_{x,y,z} &: \text{line of sight vector in ECI coordinates} \\ &= X^i_{x,y,z} - X_{x,y,z} \end{aligned} \tag{7}$$

$$f_{C/A} : \text{frequency of C/A code, } 1.023\ (MHz)$$

$$f_{L1} : \text{frequency of L1 carrier, } 1575.42\ (MHz)$$

As shown above, the received GPS signal can be described by the channel parameters $(f^i_{code,k}, \phi^i_{code,k}, f^i_{carr,k}, \phi^i_{carr,k})$ which are intimately related to the Receiver state $X$ through line of sight projections. While the received GPS signal can be described by the Receiver state, the signal replica can be generated from the Receiver state. The objective in DTE is then to search for the best estimate of the Receiver state that produces the signal replica giving rise to the highest correlation against the received signal. As for the databit sequence $D^i(t)$, our research platform, PyGNSS performs databit wipeoff with 20ms coherent integrations.

The four-step process that begins the search for the best estimate of the Receiver state is given in Fig.1. The first step is performing the correlations and FFTs. To speed up the search process, we split the underlying parameter set into two: $c\delta t$ and $c\dot{\delta t}$. The correlations help search through $c\delta t$, while the FFT spectrums help search through $c\dot{\delta t}$. As such, carrier wipeoff is performed before the correlations and code wipeoff is performed before the FFTs. The second step is generating the candidate timing error vectors. The third step is assigning values from the correlations and FFT spectrums to the respective candidate timing error vectors. The fourth step estimates the error vector $e$ as the weighted mean of the candidate timing error vectors. The error vector and the error noise covariance matrix $W$ are then used as inputs into the joint timing and tracking Extended Kalman Filter (EKF). Fig.2 describes the processes involved in the EKF two-step update process. The EKF measurement update and time update equations are also given as follows:

The EKF measurement update at epoch $k$:

$$\begin{aligned} e &: \text{error input vector} \\ &= [\Delta c\delta t, \Delta c\dot{\delta t}]^T \end{aligned} \tag{8}$$

$$W : \text{error noise covariance input matrix} \tag{9}$$

$$\begin{aligned} K &: \text{Kalman gain matrix} \\ &= \hat{\Sigma}_k H^T (H\hat{\Sigma}_k H^T + W)^{-1} \end{aligned} \tag{10}$$

$$\begin{aligned} \Delta X &: \text{state error vector} \\ &= Ke \end{aligned} \tag{11}$$

$$\hat{\Sigma}_k : \text{predicted state error covariance matrix}$$

$$\begin{aligned} H &: \text{geometry matrix} \\ &= I_2, \text{2x2 identity matrix} \end{aligned} \tag{12}$$

$$\begin{aligned} X_k &: \text{corrected state vector} \\ &= \hat{X}_k + \Delta X \end{aligned} \tag{13}$$

$$\begin{aligned} \Sigma_k &: \text{corrected state error covariance matrix} \\ &= (I - KH)\hat{\Sigma}_k \end{aligned} \tag{14}$$

The error noise covariance input matrices are estimated using 20 past error input vectors. The coherent integration and EKF update interval, $\Delta T$, are the same and set to $\Delta T = 0.020s$. PyGNSS performs navigation bit wipe-off.

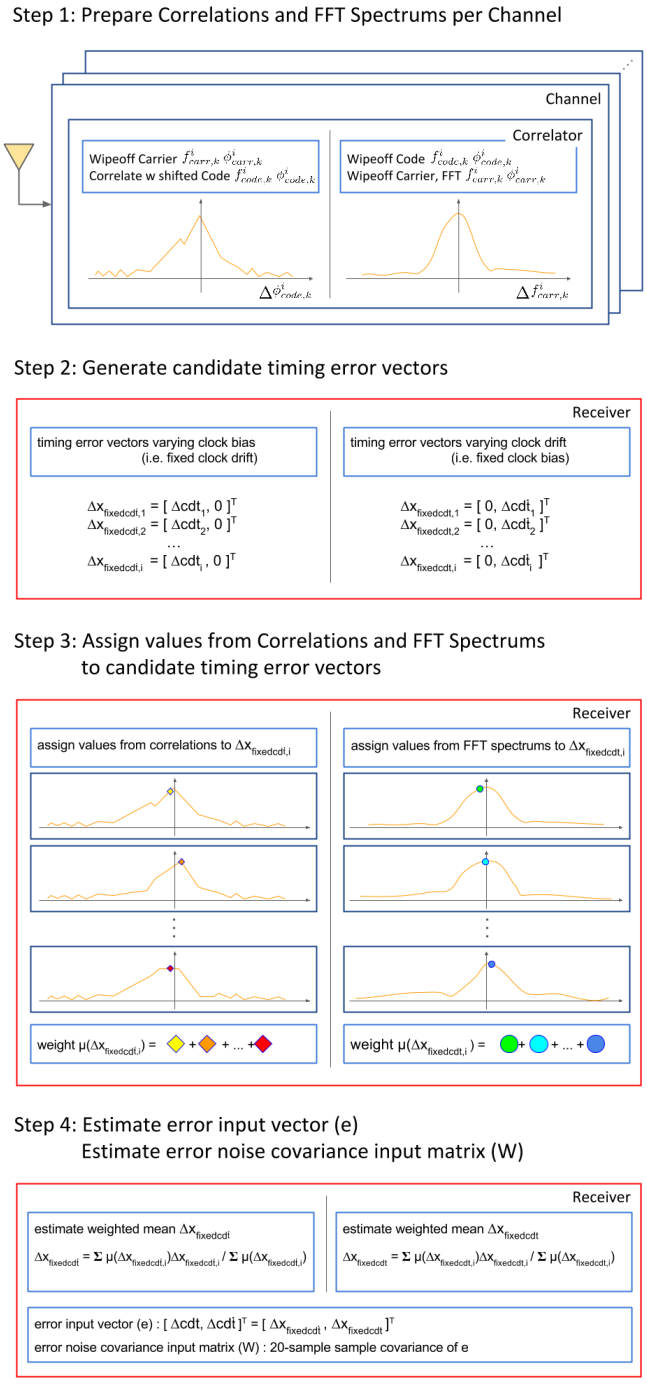


Fig. 1. Obtaining the error input vector $e$ and error noise covariance matrix $W$ via a 4-step process.

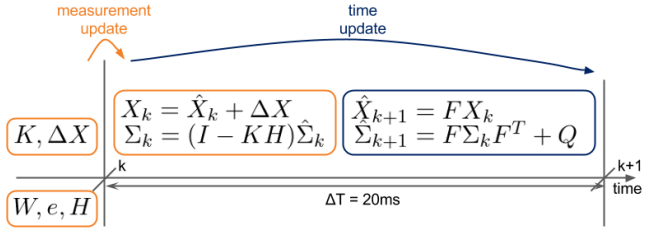


Fig. 2. Timeline of the processes involved in the EKF two-step update process.

The EKF time update equations at epoch $k+1$:

$$\hat{X}_{k+1} : \text{predicted state vector} \tag{15}$$
$$= FX_k$$
$$\hat{\Sigma}_{k+1} : \text{predicted state error covariance matrix} \tag{16}$$
$$= F\Sigma_k F^T + Q$$
$$F : \text{state propagation matrix} \tag{17}$$
$$= F(\Delta T)$$
$$= \begin{bmatrix} 1 & \Delta T \\ 0 & 1 \end{bmatrix}$$

$$\Delta T : \text{update interval, } 0.020\ (s) \tag{18}$$
$$Q_k : \text{state process noise covariance matrix} \tag{19}$$
$$= F \begin{bmatrix} 0 & 0 \\ 0 & (c \times \sigma_\tau)^2 \end{bmatrix} F^T$$
$$\sigma_\tau : \text{allan deviation of the frontend oscillator, } (s)$$

### B. DTE with Vector Discriminator and Control Loop Filter

DTE with the vector discriminator is a special and simplified case of DTE with the vector correlator. It uses only 4 candidate timing error vectors: 'Early', 'Late', 'Fast' and 'Slow', where 'Early' and 'Late' varies $c\delta t$ while 'Fast' and 'Slow' varies $c\delta\dot{t}$ . It works similar to Delay Lock Loop's (DLL) Early-Late (E-L) code phase error discriminator and Frequency Lock Loop's (FLL) carrier frequency error discriminator. The discrimination results in the $c\delta t$ and $c\delta\dot{t}$ domain can then be passed into the EKF or two simple control loop filters similar to DLL and FLL.

## III. Experiment and Analysis

This section describes the experiments performed using the first implementation (II-A) of DTE. We are still in the process of analysing the data from the alternative implementation (II-B) of DTE.

### A. Experiment Setup

In this paper, we verify the robustness of DTE via the simulation of malicious activities in the signal environment. Among many different types of attacks, we have chosen to simulate meaconing and jamming to demonstrate the ability of DTE to mitigate these intrusions. A data set is first collected under benign, open sky conditions then processed to simulate attacks. This attacked signal is then fed into both DTE and traditional tracking algorithms for performance comparison. The "severity" of the attacks was systematically adjusted and the results evaluated.

Data collection was done on the roof of Talbot Laboratory, University of Illinois, using a Universal Software Radio Peripheral (USRP) connected to a Chip-Scale Atomic Clock (CSAC), with which the raw complex voltage is recorded and prepared for post-processing. Fig.3 Data processing in software was conducted using our research platform - PyGNSS.

The interference simulation process is laid out as follows:

- **Meaconing**: A meaconing attack is simulated by generating a superposition of the original signal with a delayed

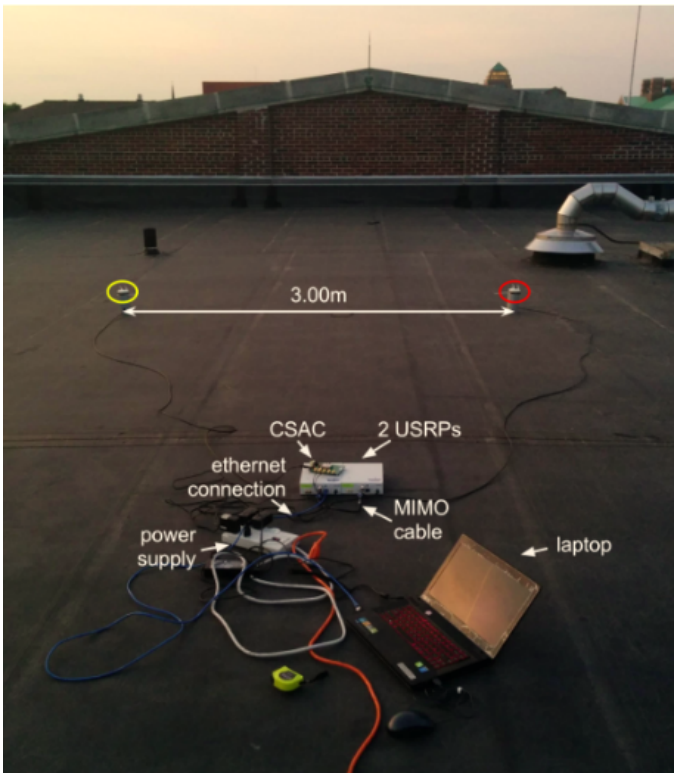


Fig. 3. Data collection equipment; only the red receiver is in use.

version of the same signal, creating a conflicting time-of-arrival (TOA). The strength of the meaconing attack is adjusted by varying the power ratio between the original signal and the delayed version.

- **Jamming**: To simulate jamming, a random complex voltage $V = A\cos\Phi + jA\sin\Phi$ is added to the original signal, where $A \sim N(0, \sigma_A)$ and $\Phi \sim U(0, 2\pi)$. This white noise with a varying standard deviation of amplitude $\sigma_A$ adjusts the level of jamming, from fairly light to irrecoverably severe.

### B. Results and Analysis

Fig.4 depicts the ability of both DTE and the traditional scalar tracking algorithm to track the frequencies of code, $f_c$ and carrier, $f_i$. As the signals are "clean" and not tampered with, it can be observed that both $f_c$ and $f_i$ converge to an oscillation within a small range shortly after the receiver launch at $t_0 = 36s$. We would like to point out that the noise seen in the scalar tracking plot is due to a shorter coherent integration period of 1ms as compared to 20ms used in DTE. In a revised draft, we would use 20ms coherent integration period for both algorithms.

Before the impact brought by meaconing and jamming attacks is analysed, one last note goes to the choice of data; that is, for the remainder of the paper, Fig.4 included, we use PRN 7 to demonstrate the frequency tracking aspect of the receivers' performances. This is done without loss to generality as all PRNs have demonstrated similar behaviour in our experiment settings. We may now proceed.

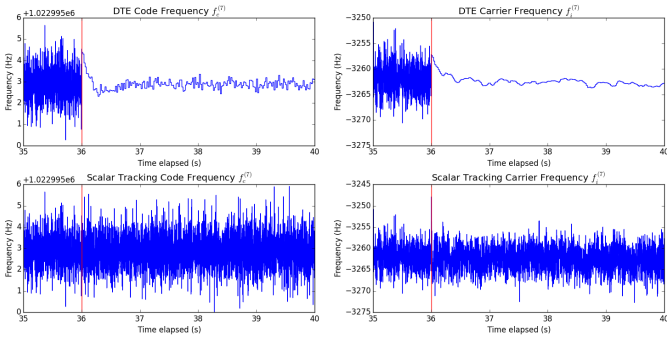


Fig. 4. Doppler frequencies are easily tracked with both DTE and scalar tracking when interference is absent. Shown above are the doppler frequencies for PRN 7. The red line symbolizes the launch of the receiver $t_0$.

*1) Meaconing:* In our paper, the meaconing attacks are simulated by shifting the clean signal, collected on the roof, by 3 samples (with the 5MHz sampling rate this is roughly equivalent to 180m) and overlapping it with the original signal. That is, the receiver will receive 2 completely identical signals, 0.6 microseconds apart. We then give this attack signal varying gains $G$ and evaluate how well DPE and scalar tracking reject these intrusions. 5 shows the frequency tracking process of both DTE and traditional scalar tracking. After the launch of the receiver at $t_0 = 36s$, a few traces, such as an increasing amplitude of oscillation and sudden spikes, provide us with hints that scalar tracking may already be operating under stress. On the other hand, there are no such signs for DTE.

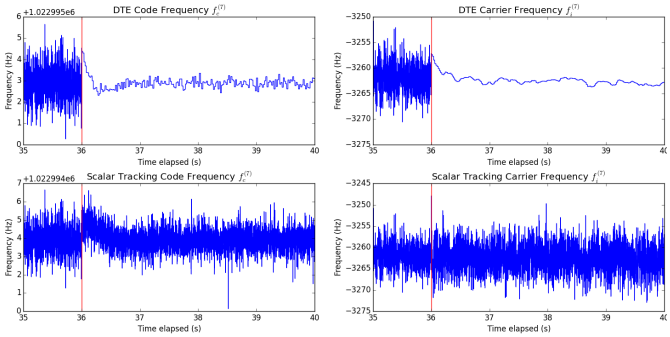


Fig. 5. Meaconing attack with gain $G = 0.5$. Minor irregularities can be observed in the scalar tracking plot.

As the attack gain is increased to 0.85, shown in Fig.6, those irregularities becomes more apparent, and to the extent that the performance of a traditional GPS receiver would start to suffer. On the other hand, the frequency tracking conducted by the DTE has been largely unaffected.

Indeed, frequency tracking is only one aspect of the generation of a timing solution, and the picture is not full without examining the correlogram of the vector correlator, shown in Fig.7 and Fig.8, from which we conclude that the DTE would still be capable of generating a correct timing solution since the correlation peak is still situated at the origin, suggesting no error. In addition, also noticeable from the correlogram of the vector correlator is the meaconing attack near 180m for the

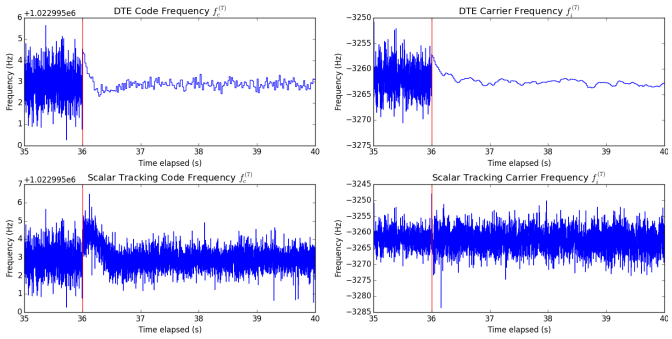


Fig. 6. Meaconing attack with gain $G = 0.85$. More irregularities are now present.

0.6 microseconds delay of the meaconing signal. This makes the confident early detection of meaconing possible.

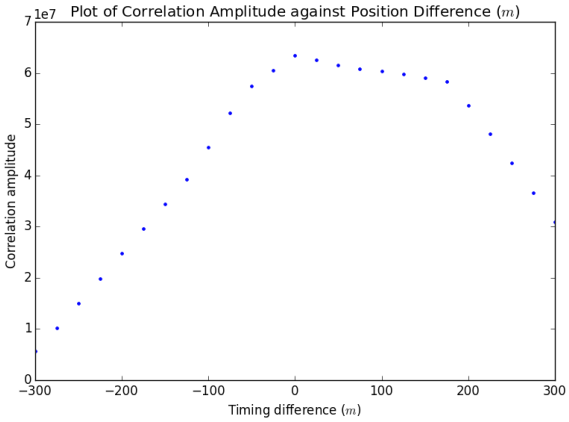


Fig. 7. Correlation peak for clock bias remains correct under meaconing attack with gain $G = 0.85$. Also noticeable from the above plot is the meaconing attack near 180m for the 0.6 microseconds delay of the meaconing signal.

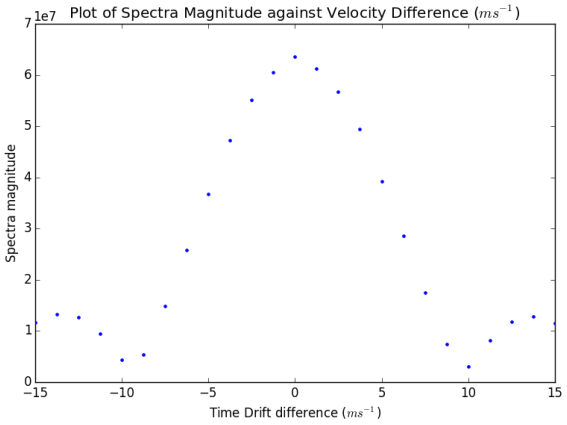


Fig. 8. Spectra peak for clock drift is unaffected by the meaconing attack with gain $G = 0.85$. The meaconing signal does not contain a difference in time drift. The spectra was also generated with code wipeoff based on the current clock bias which is the tracked non-meaconed clock bias.

*2) Jamming:* The addition of jamming signals onto our clean signal has created a similar outcome as the meaconing case. As the signal-to-noise ratio drops to zero (*ie.* the jamming noise carries approximately the same energy as the signal itself), the traditional method, scalar tracking, starts to lose track of the code and carrier frequencies, $f_c$ and $f_i$. This is shown in Fig.9, where it can be observed that the jamming noise was carried over to the frequency measurements after the receiver launch at $t_0 = 36s$.

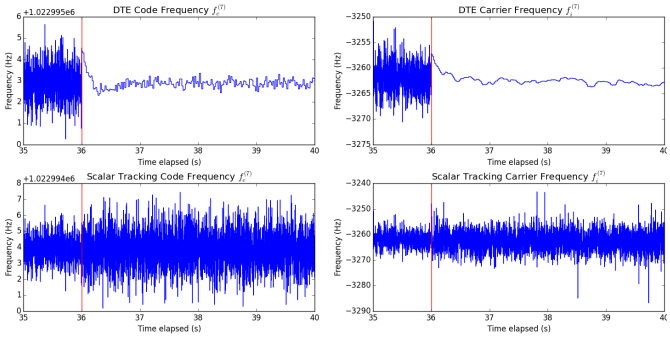


Fig. 9. Observed noisy frequency measurements for scalar tracking when jamming $SNR \approx 0dB$

Scalar tracking was unable to track the code and carrier frequencies as the signal environment turns more hostile; Fig.10 Fig.11, and Fig.12 all corroborate this point as the values of $f_c$ and $f_i$ become more noisy and diverged from the accurate values; in contrast, the DTE produces a consistent tracking performance even under these challenging circumstances.

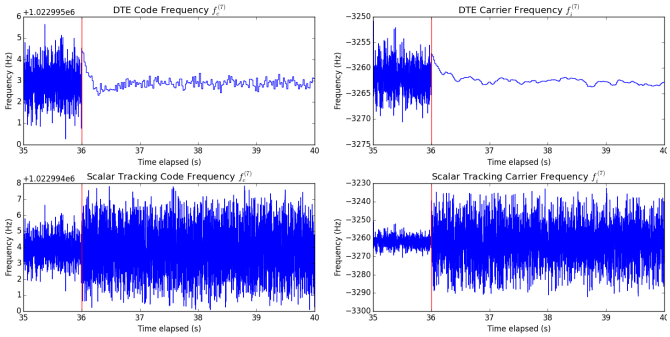


Fig. 10. Jamming attack with $SNR \approx -5dB$

It is worth noting that the frequency tracking diverges more rapidly under jamming attacks than under meaconing ones, since in our experiments, meaconing attacks are simply "replaying" the original signal with a short delay, and the Doppler frequency would thus not change considerably over that period of time; on the other hand, jamming attack is the addition of a white noise, and the frequency tracking ability for traditional receivers is hence dramatically degraded. Similar to the previous demonstrations, the DTE correlograms are shown to certify its ability to properly generate navigation solutions in these challenging scenarios.

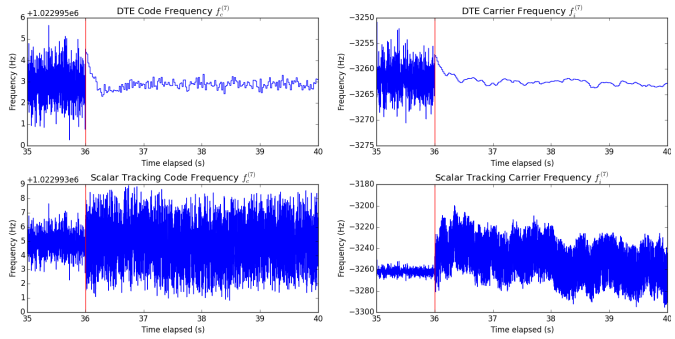


Fig. 11. Jamming attack with $SNR \approx -10dB$

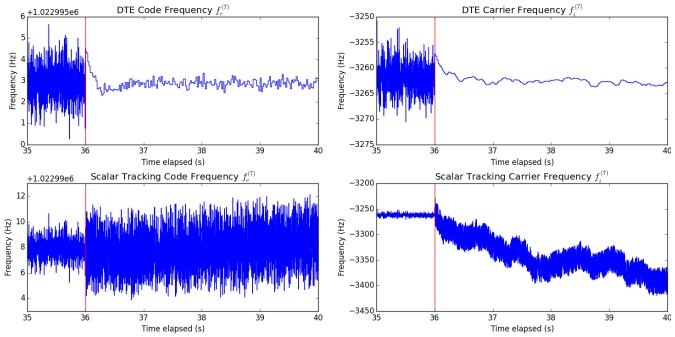


Fig. 12. Jamming attack with $SNR \approx -15dB$

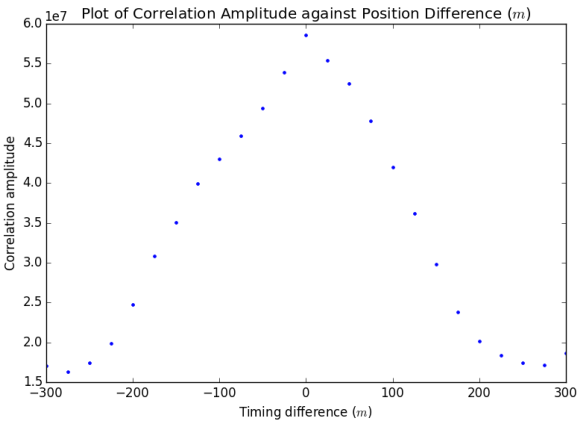


Fig. 13. Correlation peak for timing difference under $SNR \approx -10dB$

## IV. Conclusion

In summary, GPS time synchronized PMU measurements are a great aid to the control and analysis of the electrical power grid. However, this also presents a mode of attack on the power grid through disrupting the GPS time synchronization. As such, PMU measurements are not used in the direct, real-time control of the power grid.

For this reason, we present Direct Timing Estimation (DTE) for the reliable, robust and secure GPS-based time transfer to PMUs. In order for this to be a viable practical solution, we proposed a novel, effective and efficient implementation

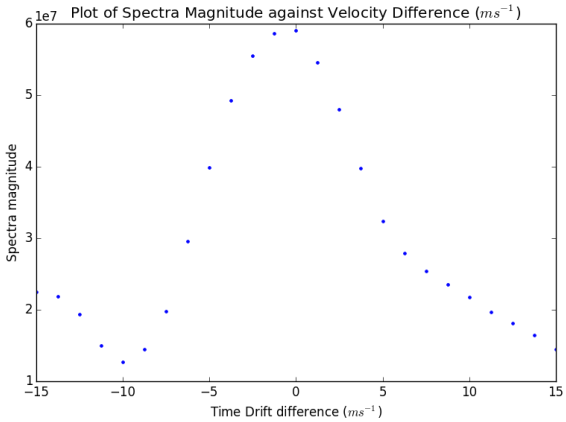


Fig. 14. Spectra peak for time drift under $SNR \approx -10dB$

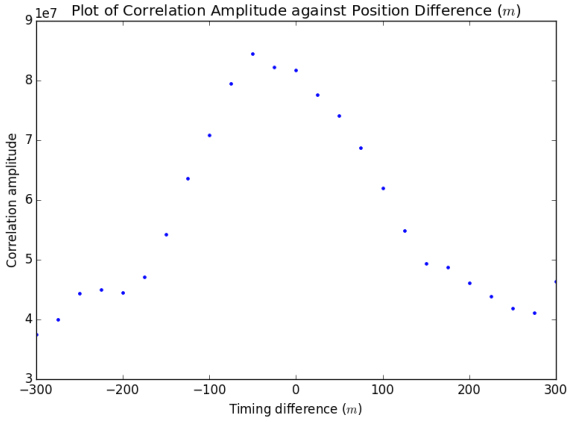


Fig. 15. Correlation peak for timing difference under $SNR \approx -15dB$

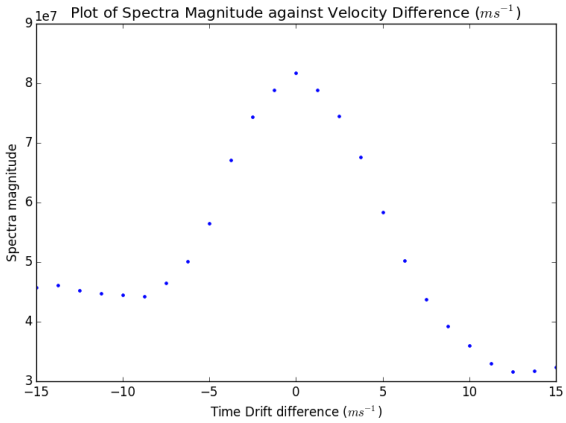


Fig. 16. Spectra peak for time drift under $SNR \approx -15dB$

of DTE. Following that, we demonstrated DTE's robustness to hostile attacks as compared to traditional scalar tracking through experimental simulations. DTE remains operational when traditional scalar tracking fails to generate the accurate timing solution.

## ACKNOWLEDGMENT

This material is based upon work supported by the Department of Energy under Award Number DE-OE0000780.

## DISCLAIMER



## REFERENCES

[1] A. Ramesh Kumar, "Direct position tracking in gps using vector correlator," Master's thesis, University of Illinois at Urbana-Champaign, 2015.

[2] J. J. Brewer, "The differential vector phase-locked loop for global navigation satellite system signal tracking," Ph.D. dissertation, AIR FORCE INSTITUTE OF TECHNOLOGY, 2014.

[3] P. Axelrad, B. K. Bradley, J. Donna, M. Mitchell, and S. Mohiuddin, "Collective detection and direct positioning using multiple gnss satellites," *Navigation*, vol. 58, no. 4, pp. 305–321, 2011.

[4] P. Axelrad, J. Donna, and M. Mitchell, "Enhancing gnss acquisition by combining signals from multiple channels and satellites," in *Proceedings of the 22nd International Technical Meeting of The Satellite Division of the Institute of Navigation (ION GNSS 2009)*, 2001, pp. 2617–2628.

[5] P. Closas, C. Fernández-Prades, J. Fernández-Rubio *et al.*, "Maximum likelihood estimation of position in gnss," *Signal Processing Letters, IEEE*, vol. 14, no. 5, pp. 359–362, 2007.

[6] P. Closas, C. Fernandez-Prades, J. Fernández-Rubio *et al.*, "Cramér–rao bound analysis of positioning approaches in gnss receivers," *Signal Processing, IEEE Transactions on*, vol. 57, no. 10, pp. 3775–3786, 2009.

[7] ——, "A bayesian approach to multipath mitigation in gnss receivers," *Selected Topics in Signal Processing, IEEE Journal of*, vol. 3, no. 4, pp. 695–706, 2009.

[8] L. R. Paulo Esteves, Mohamed Sahmoudi, "Collective detection of multi-gnss signals," *InsideGNSS*, pp. 54–65, may 2014.

[9] F. D. Nunes, J. Marcal, and F. M. Sousa, "Low-complexity vdll receiver for multi-gnss constellations," in *Satellite Navigation Technologies and European Workshop on GNSS Signals and Signal Processing (NAVITEC), 2010 5th ESA Workshop on*. IEEE, 2010, pp. 1–8.

[10] J. James Spilker, "Generalized vector processing," jul 2011, eSA International Summer School on Navigation Satellite Systems, Stanford University.

[11] ——, "Vector tracking of composite signals," jul 2011, aA272D Lecture no.5.

[12] A. J. Weiss, "Direct position determination of narrowband radio frequency transmitters," *Signal Processing Letters, IEEE*, vol. 11, no. 5, pp. 513–516, 2004.

[13] J. Liu, X. Cui, M. Lu, and Z. Feng, "Direct position tracking loop based on linearised signal model for global navigation satellite system receivers," *IET Radar, Sonar & Navigation*, vol. 7, no. 7, pp. 789–799, 2013.

[14] ——, "Vector tracking loops in gnss receivers for dynamic weak signals," *Systems Engineering and Electronics, Journal of*, vol. 24, no. 3, pp. 349–364, 2013.

[15] J. W. Cheong, J. Wu, A. G. Dempster, and C. Rizos, "Efficient implementation of collective detection," in *IGNSS symposium*, 2011, pp. 15–17.

[16] ——, "Assisted-gps based snap-shot gps receiver with fft-accelerated collective detection: Time synchronisation and search space analysis," in *25th International Technical Meeting of the satellite Division of the Institute of Navigation (ION GNSS 2012), Nashville USA*. Citeseer, 2012, pp. 2357–2370.

[17] R. DiEsposti, "Gps prn code signal processing and receiver design for simultaneous all-in-view coherent signal acquisition and navigation solution determination," in *Proceedings of the 2007 National Technical Meeting of The Institute of Navigation*, 2001, pp. 91–103.

[18] Y. Ng and G. X. Gao, "Advanced multi-receiver vector tracking for positioning a land vehicle," in *Proceedings of the 26th International Technical Meeting of the Satellite Division of the Institute of Navigation (ION GNSS+ 2014), Tampa, Florida*, 2015.

[19] ——, "Advanced multi-receiver position-information-aided vector tracking for robust gps time transfer to pmus," in *Proceedings of the 26th International Technical Meeting of the Satellite Division of the Institute of Navigation (ION GNSS+ 2014), Tampa, Florida*, 2015.

[20] S. Bhattacharyya, "Performance and integrity analysis of the vector tracking architecture of gnss receivers," Ph.D. dissertation, University of Minnesota, 2012.

[21] R. E. Kalman *et al.*, "Contributions to the theory of optimal control," *Bol. Soc. Mat. Mexicana*, vol. 5, no. 2, pp. 102–119, 1960.

[22] R. E. Kalman, "A new approach to linear filtering and prediction problems," *Journal of Fluids Engineering*, vol. 82, no. 1, pp. 35–45, 1960.

[23] E. Kaplan, C. Hegarty, P. Ward, and J. Betz, *Understanding GPS: Principles and applications 2nd ed*. Boston: Artech House, 2006, ch. Chapter 5: Satellite Signal Acquisition, Tracking, and Data Demodulation, pp. 153–240.

[24] F. D. Busse, J. P. How, and J. Simpson, "Demonstration of adaptive extended kalman filter for low-earth-orbit formation estimation using cdgps," *Navigation*, vol. 50, no. 2, pp. 79–93, 2003.

[25] Mathworks. (2015, jun) State estimation using time-varying kalman filter. [Online]. Available: http://www.mathworks.com/help/control/getstart/estimating-states-of-time-varying-systems-using-kalman-filters.html

[26] Microsemi. (2015, jun) Quantum chip scale atomic clock product info. [Online]. Available: http://www.microsemi.com/products/timing-synchronization-systems/csac#product-info

[27] P. Misra and P. Enge, *Global Positioning System: Signals, Measurements and Performance Second Edition*. Lincoln, MA: Ganga-Jamuna Press, 2006.

[28] P. Ward, "The natural measurements of a gps receiver," in *Proceedings of the 51st Annual Meeting of the Institute of Navigation*, 1995, pp. 67–85.

[29] P. W. Ward, "Performance comparisons between fll, pll and a novel fll-assisted-pll carrier tracking loop under rf interference conditions," in *Proceedings of the 11th International Technical Meeting of the Satellite Division of The Institute of Navigation (ION GPS 1998)*, 1998, pp. 783–795.

[30] P. W. Ward and T. D. Fuchser, "Stability criteria for gnss receiver tracking loops," *Navigation*, vol. 61, no. 4, pp. 293–309, 2014.

[31] N. Ashby and M. Weiss, *Global Position System Receivers and Relativity*. US Department of Commerce, Technology Administration, National Institute of Standards and Technology, 1999.

[32] M. S. Braasch and A. Van Dierendonck, "Gps receiver architectures and measurements," *Proceedings of the IEEE*, vol. 87, no. 1, pp. 48–64, 1999.

[33] Antcom. (2015, jun) P/n: 3gnssa4-xt-1. [Online]. Available: http://www.antcom.com/documents/catalogs/Page/3GNSSA4-XT-1_GNSSAntennas1.pdf

[34] E. Research. (2015, jun) Usrp n210. [Online]. Available: http://www.ettus.com/product/details/UN210-KIT

[35] ——. (2015, jun) Dbsrx2 800-2300 mhz rx. [Online]. Available: http://www.ettus.com/product/details/DBSRX2

[36] O. Shine. (2016, jan) Gps/gsm antenna/ant-555. [Online]. Available: http://www.onshine.com.tw/product_cg135940.html

[37] U. of Colorado at Boulder. (2016, jan) Sige gn3s sampler v2 usb front-end. [Online]. Available: https://ccar.colorado.edu/gnss/files/SE4110L_Datasheet_Rev3.pdf
[38] Google. (2016, jan) Google maps javascript api. [Online]. Available: https://developers.google.com/maps/documentation/javascript/
[39] ——. (2016, jan) Google streetview api. [Online]. Available: https://developers.google.com/maps/documentation/streetview/